

**EXPERIMENTAL STUDIES OF Mg- and Fe- CARBONATE PRECIPITATION AND THEIR APPLICATION TO JEZERO CRATER** M. M. Morris<sup>1</sup> and J. A. Hurowitz, <sup>1</sup>Department of Geosciences, Stony Brook University, StonyBrook, NY ([madison.morris@stonybrook.edu](mailto:madison.morris@stonybrook.edu))

**Introduction:** Analysis of spectroscopic and imaging data collected from orbit over Jezero crater, the landing site of the Mars 2020 rover, indicates that carbonate minerals are present in rocks within the crater in depositional settings that are consistent with a lacustrine origin [1]. These carbonates are dominated by Mg-carbonates magnesite and hydromagnesite and show evidence for Ca- and Fe-substitution [1]. The compositions of these carbonates have been found to be very similar to the carbonate minerals in the Martian meteorite Allan Hills 84001 (ALH 84001), which were formed at a temperature of  $18 \pm 4^\circ\text{C}$  [2]. Beyond constraints on precipitation temperature, the environmental conditions in which the ALH 84001 carbonates were formed is relatively unconstrained, leaving a knowledge gap in our understanding of the fluid chemical conditions that could have given rise to these precipitates. Further, Mg-rich carbonates are less common on Earth than Ca- and Fe-carbonates, resulting in a lack of understanding about what they can reveal regarding surface paleoenvironmental conditions.

Understanding the conditions in which Martian minerals, specifically Mg-rich carbonates, were formed can provide insight on pH, temperature, fluid composition, and precipitation pathway. The C- and O- isotopic composition of Mg-carbonate minerals can also be exploited to reveal the geobiological history of Mars [3], provided that we understand the abiotic processes that can also give rise to such minerals.

Here, we present the results of experiments designed to precipitate magnesite and siderite in Mg-Fe-Ca compositional space, with the goal of understanding the fluid chemical conditions that gave rise to carbonates found in the ALH 84001 meteorite [4], which are potentially analogous to carbonates that will be analyzed by the Mars 2020 rover.

**Experimental Methods:** Free drift batch experiments were modeled after Romanek et. al., 2009 who precipitated carbonates in the Ca-Fe-Mg chemical system at room temperature [5]. We modeled our cation and dissolved inorganic carbon (DIC) concentrations after their experiment FD-15, but in our case we have also added pH variation to our experimental design and are also evaluating how precipitates change character

as a function of time. Three groups of five samples were prepared in an anaerobic chamber where temperature remained constant at  $\sim 25^\circ\text{C}$ . Each 320 mL batch experiment contained .63 mL of 1.01 mmol  $\text{CaCl}_2$ , 22.6 mL of 0.75 mmol  $\text{MgCl}_2$ , 17.6 mL of 1.00 mmol  $\text{NaHCO}_3$ , and mmol 2.6 mL of 0.24 mmol  $\text{FeCl}_2$ . Each of the three groups was then adjusted to a pH of 7, 9, and 11, referred to as Group 7, Group 9, and Group 11 (G7, G9, G11, respectively). The first of the five samples within a group would be analyzed 24 hours after precipitates were first observed, with the remaining four samples being collected after 48 hours, 1 week, 1 month, and 2 months. Precipitates were collected via vacuum flask inside the anaerobic chamber and left overnight to dry in a vacuum desiccation chamber. The following day, samples were ground into a fine powder, rinsed with Milli-Q water and left in the anaerobic chamber until they were dry. Samples were then characterized by X-ray diffraction (XRD) and combined Scanning Electron Microscopy-Energy Dispersive X-ray spectroscopy (SEM-EDX).

**Results:** G9 and G11 formed precipitates almost immediately after solution mixing. G7 did not begin to form precipitates until a week after mixing and at the time of this abstract have not formed enough to be characterized by XRD or SEM. While solutions for G7 varied in color, remaining clear hues of yellow and green throughout the experiment, G9 and G11 solutions were mostly clear and contained abundant opaque white precipitates. Thus far, we have collected 5 precipitate samples from each of the G9 and G11 batch experiments, corresponding to 24 hour to 2 month time intervals. Upon filtering, the G11 samples exhibited the same opaque white color they had in solution, and dried as a varying cream/yellow hue. The G9 samples presented as a pale blue when wet and dark green/brown when dry, consistent with the possibility that this precipitate incorporated more iron.

SEM images show that G9 contains a diversity of precipitate morphologies, including blocky forms, rods and spheres (Fig.1A). G11, while also containing an abundance of blocky shapes, had small spherical blebs attached to the surface of the blocky precipitates, as opposed to separate rods and spheres (Fig.2A).

For the G9 precipitates, the XRD patterns change with time from a featureless pattern consistent with an amorphous precipitate, and progressively change to a pattern that has XRD peaks consistent with nesquehonite  $\text{Mg}(\text{HCO}_3)(\text{OH}) \cdot 2(\text{H}_2\text{O})$  and calcite. EDS analyses collected in association with SEM images reveal that the blocky G9 precipitates are an iron bearing magnesium carbonate, suggesting that the nesquehonite formed in our experiments contains iron. EDS analysis also reveals that the spherical precipitates observed in SEM are calcite (Fig. 1B).

XRD analysis of G11 precipitates reveals that the materials formed in these experiments have broad XRD reflections. While over time some peaks become more distinct, they remain difficult to identify. SEM-EDS analysis indicates the majority of material derived from the G11 experiments is magnesium rich, possibly an Mg-carbonate or Mg-hydroxide, and that the small spherical grain attached to larger blocky precipitates are Ca-bearing, possibly calcite (Fig.2B). We note that calcite is not obviously present in the XRD patterns from the G11 series, possibly as a result of a lower abundance, consistent with qualitative SEM observations that indicate this is a minor phase.

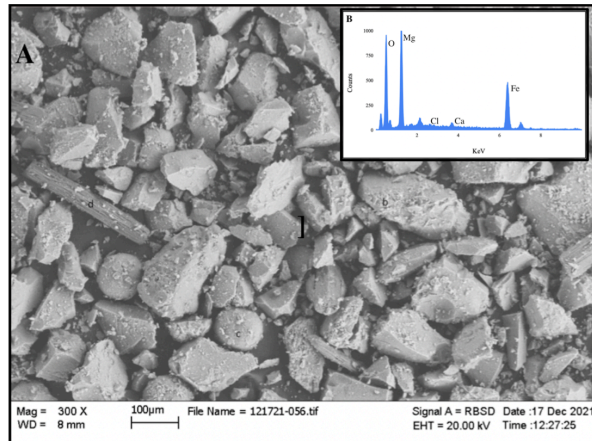


**Figure 1:** A) SEM image of G9 containing the three noted morphologies; blocky forms, rods, and spheres. B) Average SEM data found in G9.

**Discussion:** The constraints given by Romanek et al., 2009, as well as saturation state calculations conducted using the Spec8 subroutine in Geochemist's Workbench before experiment implementation suggest that carbonates similar to those found in ALH 84001 [2,5] should form in all of our experiments, regardless of initial pH. While magnesium carbonates and iron bearing magnesium carbonates are observed through-

out the experiment, the expected siderite and magnesite did not precipitate. Notably, iron only clearly precipitated in G9 while it stayed in solution for G11. The varying factor of time in our experiments allows constraints to be placed on the time scales required for precipitate mineralogy to evolve. After 24 hours, the first set of precipitates for each group were amorphous, and became more crystalline as time progressed. The difference between expected and observed precipitates highlights the impact pH has on fluid chemistry and mineral precipitation pathway when all other fluid chemical parameters are the same. Our experimental results can be used as a basis for comparison to the Jezero carbonate record to better understand the conditions of carbonate mineralization.

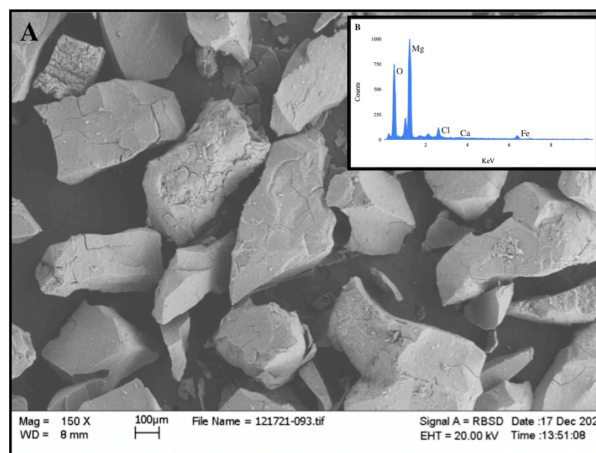


**Figure 3:** SEM image of G11 containing the noted morphologies; blocky forms with small spherical inclusions. B) Average SEM data found in G11.

**Future Work:** G7 will be analyzed in the same manner as the other groups when enough precipitates have been produced. We will utilize other tools such as Fourier Transform Infrared Spectroscopy (FTIR) and Electron Backscatter Diffraction (EBSD) to help identify constraints on the requirements for cation substitution in iron and magnesium carbonates. It is our goal to measure the C-, O- and clumped isotope ratios of the experiment in order to evaluate how temperature, evaporation, degassing, and super-saturation has on the isotopic composition.

**References:** [1] Horgan, B. et al. (2020) *Icarus*, 339, 1243480. [2] Halevy, I. et al (2011) *PNAS*, 108, 16895-16899. [3] Valley, J. et al. (1997) *Science*, 275, 1633-1638. [4] Harvey, R. et al. (1996) *Nature*, 382, 49-51. [5] Romanek, C. et al. (2009) *ScienceDirect*, 73, 5361-5376.